Contourite processes associated with the Mediterranean Outflow Water after its exit from the Strait of Gibraltar: Global and conceptual implications

F.J. Hernández-Molina[1], E. Llave[2], B. Preu[3], G. Ercilla[4], A. Fontan[5], M. Bruno[6], N. Serra[7], J.J. Gomiz[6], R.E. Brackenridge[8], F.J. Sierro[9], D.A.V. Stow[8], M. García[10], C. Juan[5], N. Sandoval[11], and A. Arnaiz[12]

[1]Department of Earth Sciences, Royal Holloway, University of London, Egham, Surrey TW20 0EX, UK
[2]Instituto Geológico y Minero de España (IGME), Ríos Rosas 23, 28003 Madrid, Spain
[3]Chevron, Seafield House, Aberdeen AB15 6XL, UK
[4]Institut de Ciències del Mar, CSIC, Passeig Marítim de la Barceloneta 37-49, 08003 Barcelona, Spain
[5]Facultad Ciencias do Mar, Universidade de Vigo, 36200 Vigo, Spain
[6]Centro Andaluz de Ciencia y Tecnología Marinas (CACYTMAR), Universidad Cádiz, Puerto Real, 11510 Cádiz, Spain
[7]Institut für Meereskunde, Universität Hamburg, Bundesstrasse 53, 20146 Hamburg, Germany
[8]Institute of Petroleum Engineering, Heriot-Watt University, Edinburgh EH14 4AS, Scotland, UK
[9]Departamento de Geología, Universidad de Salamanca, 37008 Salamanca, Spain
[10]Instituto Andaluz de Ciencias de la Tierra (IACT), CSIC, Universidad de Granada, Avenida de las Palmeras 4, 18100 Armilla, Spain
[11]Sociedad Española de Estudios para la Comunicación Fija a través del Estrecho de Gibraltar, S.A. (SECEGSA), c/ Alfonso XII 3-5, 28014 Madrid, Spain
[12]Repsol, Méndez Álvaro 44, Edificio Azul 2ª planta, 28045 Madrid, Spain

ABSTRACT

We characterize the eastern Gulf of Cadiz, proximal to the Strait of Gibraltar, using a multidisciplinary approach that combines oceanographic, morphosedimentary, and stratigraphic studies. Two terraces (upper and lower) were identified along the middle slope. They are composed of several associated morphologic elements, including two large erosive channels, which allow us to determine a new and more detailed understanding of the Mediterranean Outflow Water (MOW) pathway and its deceleration upon exiting the Strait of Gibraltar. There is evidence for along-slope circulation and additional secondary circulation oblique to the main flow. The present upper core of the MOW flows along the upper terrace and the lower core flows along the lower terrace. However, the lower terrace shows larger and better defined erosive features on the seafloor than does the upper terrace; we attribute this to a denser, deeper, and faster MOW circulation that prevailed during past cold climates. Development of the present features started ca. 3.8–3.9 Ma, but the present morphology was not established until the late Pliocene–early Quaternary (3.2 to older than 2.0 Ma), when the MOW was enhanced, coeval with global cooling, a sea-level fall, and an increase in thermohaline circulation. We propose a direct link between the MOW and the Atlantic Meridional Overturning Circulation and therefore between the MOW and both the Northern Hemisphere and global climate. Our results have enabled a better understanding of a major overflow related to an oceanic gateway, and are of broad interest to geologists, climatologists, oceanographers, and petroleum geologists.

INTRODUCTION

Our understanding of the role of deep ocean circulation in the sedimentary evolution of continental margins is rapidly improving. However, gaining knowledge about the processes involved requires that connections be made between contourite features, their spatial and temporal evolution, and the near-bottom flows that form them. We propose a multidisciplinary approach to evaluate the present and ancient processes related to the Mediterranean Outflow Water (MOW) and its evolution in the Gulf of Cadiz after it is funneled through the Strait of Gibraltar. Morphosedimentary features are identified using swath bathymetry and seismic profiles, and their oceanographic and geologic implications are discussed. Oceanographic analysis was performed using acoustic Doppler current profiler (ADCP) and conductivity, temperature, and depth (CTD) data sets, integrated with acoustic analysis and numerical simulations. Seismic data and sediment samples collected by dredges, cores, and borehole MPC-1 provided details on sedimentology, stratigraphy, evolution, and age constraints (see Fig. DR1 in the GSA Data Repository[1]).

The Strait of Gibraltar conditions the Mediterranean-Atlantic water-mass exchange, and is one of the most important oceanic gateways worldwide. It enables the addition of highly saline MOW into the Atlantic Ocean, which enhances the density of the North Atlantic and preconditions it for deep thermohaline convection. Without the MOW, the Atlantic Meridional Overturning Circulation (AMOC) would be reduced by ~15% and the North Atlantic surface temperature would decrease by as much as 1 °C (Rogerson et al., 2012). The MOW results from the mixing of Mediterranean Levantine Intermediate Water (LIW) and Western Mediterranean Deep Water (WMDW) within the strait. Upon exiting, the MOW cascades downslope as an overflow of 0.67 ± 0.28 Sv of warm saline water (Serra et al., 2010). It flows northwestward after exiting the strait, settling as an intermediate contour current along the middle slope at water depths between 400 and 1400 m, with two differentiated cores: the upper core and the lower core (MU and ML, Fig. DR1). An extensive contourite depositional system has been generated by the interaction of the MOW and the middle slope (Hernández-Molina et al., 2008). Our work is focused on the sector of the Gulf of Cadiz after the exit from the Strait of Gibraltar (Fig. 1); this sector is characterized by an abrasional surface oriented along slope between 500 and 800 m, ~100 km long and 30 km wide, and consisting of sandy sheeted drifts, scours, ripples, sand ribbons, and sediment waves (Nelson et al., 1993).

CONTOURITE FEATURES

Erosional and depositional contourite features were identified west of the Strait of Gibraltar (Figs. 1 and 2). Two zones (eastern and western) are separated by a region of basement highs, and are coincident with a marked change in margin trend from west-southwest to northwest, as well as the development of a distinct middle slope to the west. In both zones, the upper slope is locally incised by downslope-trending valleys,

[1]GSA Data Repository item 2014080, supplemental information (Table DR1 and Figures DR1–DR4), is available online at www.geosociety.org/pubs/ft2014.htm, or on request from editing@geosociety.org or Documents Secretary, GSA, P.O. Box 9140, Boulder, CO 80301, USA.

and in the western zone a sandy plastered drift is identified. Erosional features dominate in the eastern zone, composing a large (3–4 km wide), west-southwest–trending channel (called the southern channel) located along the southern part of the strait. A smaller northern channel was also identified. In the western zone, two terraces (lower and upper) are present, each comprising (from landward to seaward) a basinward-dipping erosional surface, a channel, a smooth mounded drift adjacent to the channel, and numerous small furrows oblique to the channel.

The upper terrace is shallower in the east (500 m) and deepens northwestward (~730 m). It is 13.5–23 km wide and slopes seaward ~0.34° in the east and ~0.18° in the west. The erosional surface is a marked erosive scarp incised into the upper slope with a clear truncation surface (Fig. 2). The northern channel is filled with coarse sandy sediments and becomes more distinctive toward the northwest, where it feeds into the Cadiz and Guadalquivir contourite channels (Fig. 1). Its axis slopes from 500 m in the east to 780 m in the northwest, and it is bounded on its seaward flank by a drift. The crest of this drift also slopes, from 530 m in the east to 650 m in the west. It is constructed

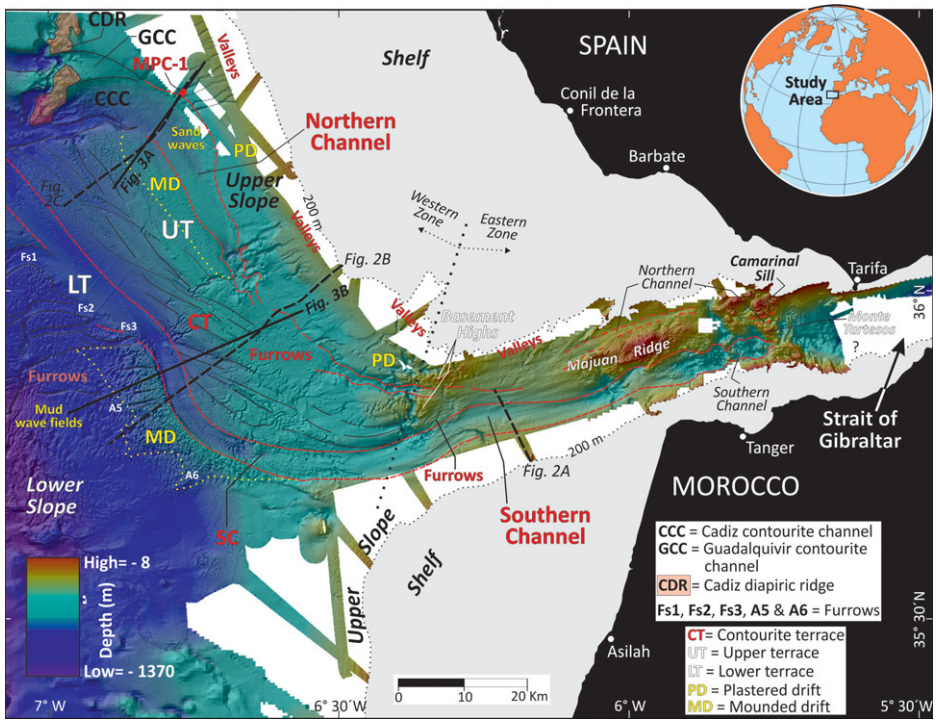

Figure 1. Swath bathymetry at exit of Strait of Gibraltar. Main depositional and erosive features are shown.

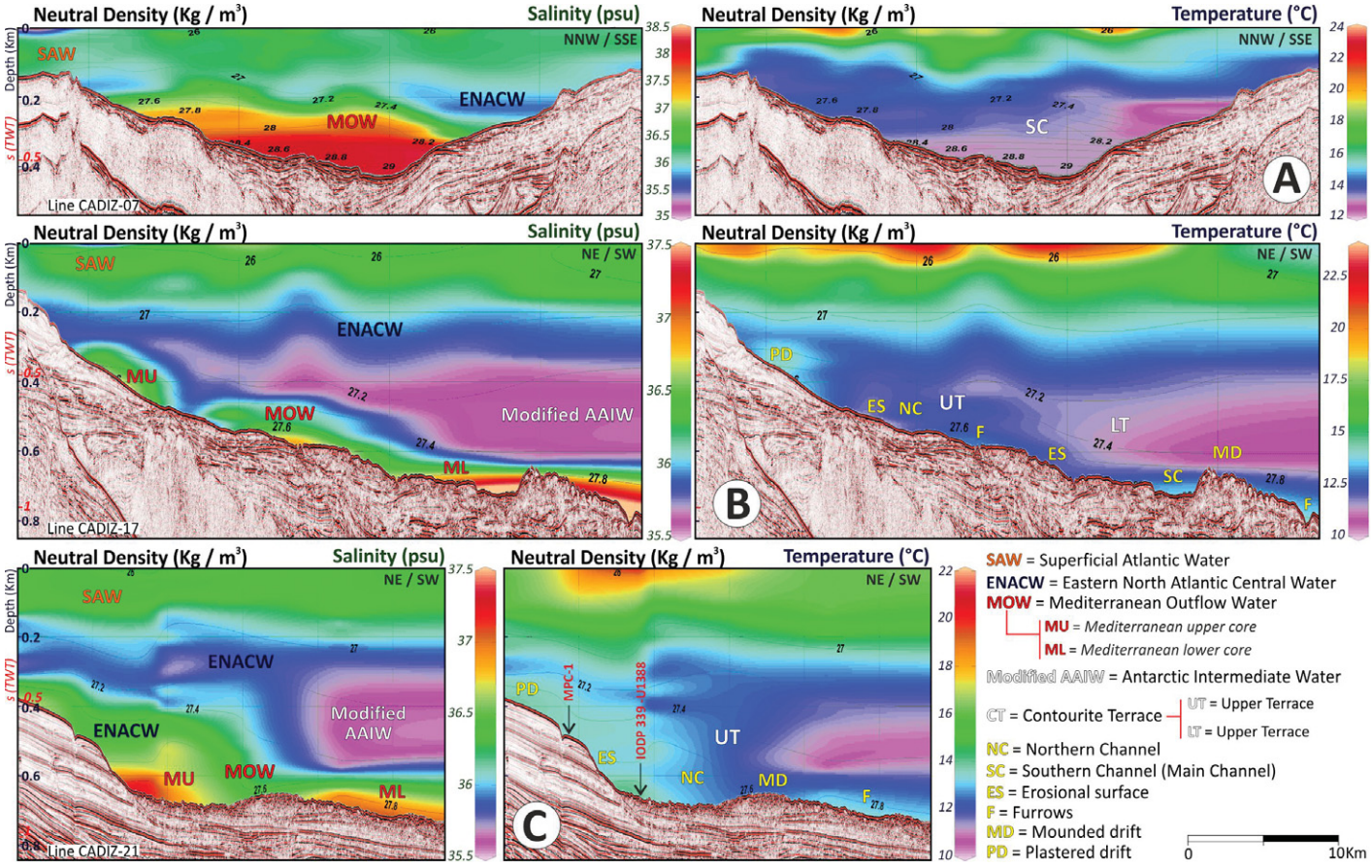

Figure 2. Seismic and hydrographic vertical sections from exit of Strait of Gibraltar. Water column colors indicate salinity (left) and temperature (right). Water-mass interpretations are shown on left sections and major contourite features are shown on right sections. Profile locations are in Figure 1. TWT—two-way traveltime.

by erosional and depositional phases having a complex internal structure composed of sandy deposits. A series of furrows deviates from the northern channel by 30°–45° (Fig. 1). The lower terrace has larger and better defined features than the upper terrace, and deepens northwestward, from 585 m in the southeast to 750 m in the northwest. This terrace is ~9 km wide and slopes seaward an average of 0.45° in the eastern sector and 0.18° in the western sector. The large and incised southern channel is ~6 km wide and is characterized by coarse to very coarse sand deposits; it has a broadly sinusoidal shape, west-southwest to northwest trend, and feeds into the Cadiz contourite channel in the central sector. The channel axis slopes from 715 m in the east to 780 m in the northwest. Seaward of the southern channel, an associated drift is characterized by irregular morphology and muddy deposits (Fig. 2). The drift has a crest that deepens westward from 600 m to ~830 m. Numerous furrows are evident across the drift, trending at 40°–45° from the channel orientation, but they evolve downslope to southwest-oriented furrows (Fs1 to Fs 3 in Fig. 1) due to the changing gradient of the lower slope.

The onset and evolution of these contourite features are based on biostratigraphic and cyclostratigraphic analysis of borehole MPC-1 (Fig. 3; Fig. DR2). The lowermost lower Pliocene seismic units are characterized by weak, aggradational reflections and consist of mud. Overlying those, an important ca. 3.8–3.9 Ma lithological change is identified, when sandier deposits become dominant. A significant regional change in both seismic facies and depositional style occurred during the late Pliocene–early Quaternary, observed in a hiatus from 3.2 Ma to younger than 2.58 Ma (the base of the Quaternary discontinuity). Quaternary deposits, characterized by interbedded sands, shell beds, silts, and clays, are clearly distinguished from the underlying Pliocene units by higher amplitude seismic reflections. After the middle Pleistocene discontinuity (ca. 0.9 Ma), the sheeted drifts become even sandier.

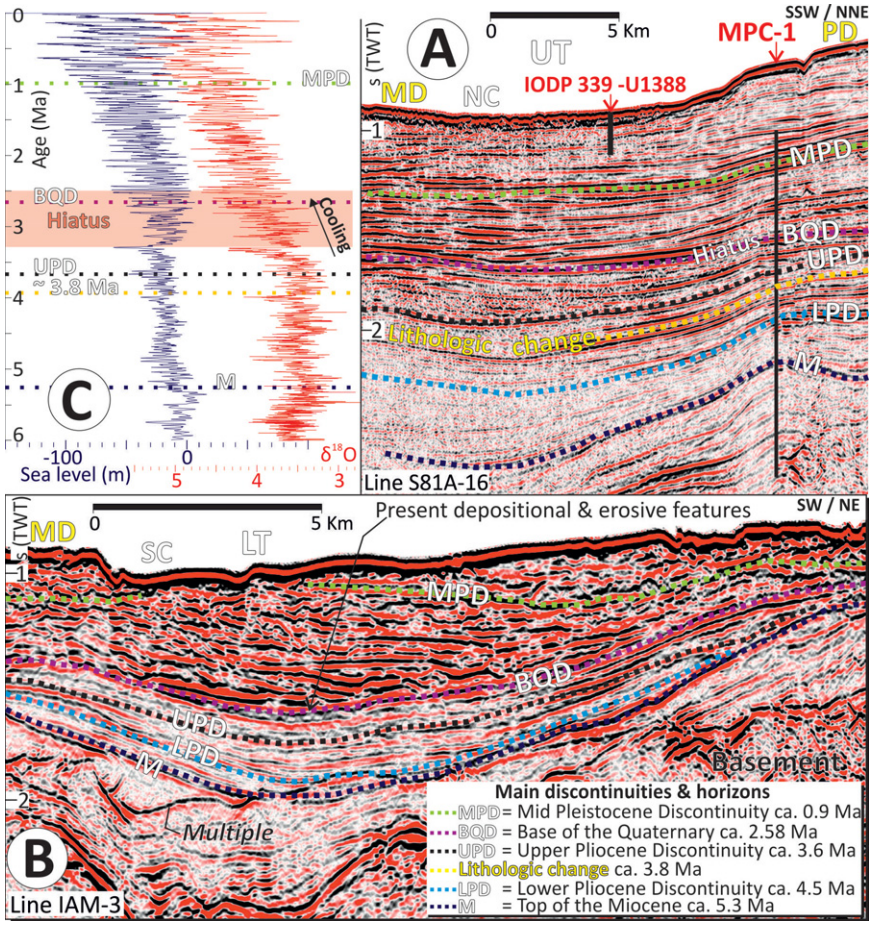

Figure 3. A, B: Multichannel seismic reflection profiles indicating main discontinuities, seismic facies, and position of well MPC-1. C: Global climatic and sea-level curves for past 6 m.y. (Miller et al., 2011). Profile locations in Figure 1; abbreviations as in Figure 2 legend. TWT—two-way traveltime.

HYDROGRAPHIC FEATURES

Five water masses were identified in the study area (Fig. 2; Fig. DR3) based on analysis of CTD and ADCP data: (1) Surface Atlantic Water (SAW); (2) Eastern North Atlantic Central Water (ENACW); (3) modified Antarctic Intermediate Water (AAIW); (4) MOW; and (5) North Atlantic Deep Water (NADW). The observed values of potential temperature (θ) and salinity (S) are similar to previously reported values (Serra et al., 2010). The dissolved oxygen (O_2) and neutral density (g^n) values are based on descriptions of Aït-Ameur and Goyet (2006) and Louarn and Morin (2011) (Table DR1 in the Data Repository). The SAW is the most superficial water mass (above 180–200 m). It circulates eastward along the northern sector toward the Alboran Sea, and through the Strait of Gibraltar, where it shallows to <100 m. The ENACW is directly below the SAW down to ~500–600 m, and also shallows in the strait to ~225 m. The MOW flows above the NADW and directly below the ENACW, but in the opposite direction, with velocities that can locally exceed 100 cm/s. The MOW upper boundary dips seaward, forming a local doming, where higher turbulence and faster flows are estimated. The MOW plume has two quasi-permanent main cores, the upper and lower, each with an overlying countercurrent, as well as smaller and less intense intermittent filaments. The modified AAIW was recently identified in the Gulf of Cadiz (Louarn and Morin, 2011), but our study presents its first record in the eastern Gulf of Cadiz, where it represents the coldest water mass above the MOW with a bottom boundary identified down to 600–625 m. This water mass also flows northwest, further confining the MOW and ENACW against the slope. Internal waves and nepheloid layers occur associated with the SAW interact with the shelf break, as well as at the interfaces between the SAW-ENACW, ENACW–modified AAIW, and along the upper boundary of the MOW.

DISCUSSION AND CONCLUSIONS

The identified major contourite features result from the MOW undergoing a marked reduction in density, increase in volume, and deceleration within the first ~100 km after its exit from the Strait of Gibraltar. Immediately west of the Camarinal Sill (Fig. 1), the MOW current velocity decreases from >240 cm/s to 60–100 cm/s further northwest, and its volume transport increases by a factor of 3 to 4 (Serra et al., 2010). The new morphosedimentary map presented here allows us, for the first time, to trace the local interaction between the MOW and the seafloor immediately downstream of Strait of Gibraltar. Close to the strait, the most significant erosional feature is the southern channel, which clearly shows that most of the MOW flows along the southern zone for ~55 km, until reaching the region of basement highs. This location marks an abrupt change in the seafloor morphology, with the development

of the upper and lower terraces along the middle slope to the west. Both terraces have similar morphologic elements moving seaward: an erosional surface, a channel, a smooth mounded drift, and furrows. The erosional surface and the channel formation result from the tendency of the Coriolis-controlled flow to be concentrated along its right side, eroding the right flank of the channel (viewed downstream) and constructing a mounded drift on the left side where the current velocity is reduced. These processes are similar to those described for the mounded drifts along other margins (Hernández-Molina et al., 2008). However, there are two intriguing differences: first, the same features are observed at two different depths; and second, the seaward occurrence of scours and furrows is oblique (30°–45°) to the channels. The feature repetition is indicative of similar processes at different depths.

As the MOW descends, the Coriolis force deflects the flow against the slope and the current axis veers northwestward. Previous studies suggest that in the central sector of the Gulf of Cadiz, the flow splits into an upper and a lower core, due to the effects of bottom friction and seafloor topography (Serra et al., 2010). The flows of the two cores have different densities, thus different depths, suggesting that their formation might require some kind of flow-stripping process. However, our results indicate that separation of current cores occurs earlier in the MOW pathway and that the erosive effects of the upper and lower cores have shaped the upper and lower terraces (and associated channels), respectively. This further implies that generation of the upper and lower cores either occurs in the central part of the Strait of Gibraltar or is directly inherited from the two principal water masses (LIW and WMDW) exiting the Alboran Sea. The largest principal erosive features and coarse sandy deposits occur on the lower terrace and along the southern channel, implying that current intensity was strongest and most persistent in this area. However, hydrographic measurements and three-dimensional numerical simulations of salinity, temperature, and current speed in the study area (Fig. 2; Figs. DR3 and DR4) show that, under the present conditions, MOW is mainly circulating along the upper terrace, with little circulation of the lower core over the lower terrace. Therefore, the erosional features along the lower terrace (erosional surface and southern channel) must have formed during a previous period of enhanced MOW, during which the lower core was dominant. Our hypothesis that the two MOW cores change in volume, density, and speed over time is consistent with (1) both terraces (and respective channels) being at different water depths; (2) paleoceanographic studies indicating that the MOW was denser and flowed deeper and faster along the Iberian margin during past cold episodes (Rogerson et al., 2012, and references therein); and (3) the existence of a broader, deeper main channel, and a narrower, shallower secondary channel within the Cadiz contourite channel in the central part of the Gulf of Cadiz (García et al., 2009), the main path for the lower core of MOW. Therefore, we propose here that the MOW upper core flows mostly along the upper slope and the upper terrace during warm highstand intervals (as at present), and that an enhanced lower core flows along the middle slope and the lower terrace during longer cool lowstand intervals. This hypothesis has important implications for the entire Atlantic Iberian margin in terms of the vertical displacement of water masses as well as changes in facies distribution. The furrows are indicative of secondary flow. Whereas the main core produces the large channel, due to bottom stress, induced MOW filaments in the bottom Ekman layer are generated at an oblique direction from the main flow (Pedlosky, 1996), thereby forming the furrows. The other across-slope channels and gullies identified over the slope indicate a more complex interference between along-slope and down-slope sedimentary processes.

The presence of extensive sand-rich deposits over contourite terraces and channels has important conceptual implications, both in establishing a facies model for sandy contourites and in assessing their potential for deep-water hydrocarbon exploration.

The opening of the Gibraltar gateway is well documented to have occurred at the end of the Miocene (Nelson et al., 1993). The main discontinuities identified in the Pliocene and Quaternary sedimentary record resulted from tectonic evolution of the margin, coupled with paleoceanographic changes in the MOW. Development of the present contourite features started ca. 3.8 Ma, when the overflow intensified and sandy contourites started to be deposited. The MOW continued to gain influence over the margin throughout the Pliocene, becoming completely dominant during the late Pliocene and early Quaternary (3.2 Ma to older than 2.0 Ma). During this period, there was a significant intensification of MOW current activity (with hiatuses formation) coeval with global cooling (Fig. 3C), sea-level fall (Miller et al., 2011), and enhanced thermohaline circulation (Rogerson et al., 2012) and AMOC (Bartoli et al., 2005). The increase in the transport of warm saline waters to northern latitudes via the MOW likely contributed to an enhanced AMOC, and consequently, to changes in the Northern Hemisphere and global climate.

ACKNOWLEDGMENTS

We are very grateful to Repsol and the Consejo Superior de Investigaciones Científicas (CSIC)–Institut Jaume Almera (geodb.ictja.csic.es) for allowing us to use an unpublished dataset. We thank A. Piola (Servicio de Hidrografía Naval, Argentina) and G. Shanmugam (University of Texas at Arlington, USA) for revising the manuscript before submission, as well as the science editor and reviewers for their suggestions, which helped us to improve the paper. This research was supported through the Ciencia y Tecnologías Marinas projects CTM 2008-06399-C04/MAR and CTM 2012-39599-C03.

REFERENCES CITED

Aït-Ameur, N., and Goyet, C., 2006, Distribution and transport of natural and anthropogenic CO_2 in the Gulf of Cádiz: Deep Sea Research Part II: Topical Studies in Oceanography, v. 53, p. 1329–1343, doi:10.1016/j.dsr2.2006.04.003.

Bartoli, G., Sarnthein, M., Weinelt, M., Erlenkeuser, H., Garbe-Schönberg, D., and Lea, D.W., 2005, Final closure of Panama and the onset of Northern Hemisphere glaciation: Earth and Planetary Science Letters, v. 237, p. 33–44, doi:10.1016/j.epsl.2005.06.020.

García, M., Hernández-Molina, F.J., Llave, E., Stow, D.A.V., León, R., Fernández-Puga, M.C., Díaz del Río, V., and Somoza, L., 2009, Contourite erosive features caused by the Mediterranean Outflow Water in the Gulf of Cadiz: Quaternary tectonic and oceanographic implications: Marine Geology, v. 257, p. 24–40, doi:10.1016/j.margeo.2008.10.009.

Hernández-Molina, F.J., Llave, E., and Stow, D.A.V., 2008, Continental slope contourites, *in* Rebesco, M., and Camerlenghi, A., eds., Contourites: Developments in Sedimentology 60: Amsterdam, Elsevier, p. 379–407, doi:10.1016/S0070-4571(08)00219-7.

Louarn, E., and Morin, P., 2011, Antarctic Intermediate Water influence on Mediterranean Sea water outflow: Deep Sea Research Part I: Oceanographic Research Papers, v. 58, p. 932–942, doi:10.1016/j.dsr.2011.05.009.

Miller, K.G., Mountain, G.S., Wright, J.D., and Browning, J.V., 2011, A 180-million-year record of sea level and ice volume variations from continental margin and deep-sea isotopic records: Oceanography, v. 24, p. 40–53, doi:10.5670/oceanog.2011.26.

Nelson, C.H., Baraza, J., and Maldonado, A., 1993, Mediterranean undercurrent sandy contourites, Gulf of Cadiz, Spain: Sedimentary Geology, v. 82, p. 103–131, doi:10.1016/0037-0738(93)90116-M.

Pedlosky, J., 1996, Ocean circulation theory: Heidelberg, Springer-Verlag, 453 p.

Rogerson, M., Rohling, E.J., Bigg, G.R., and Ramirez, J., 2012, Paleoceanography of the Atlantic-Mediterranean exchange: Overview and first quantitative assessment of climatic forcing: Reviews of Geophysics, v. 50, RG2003, doi:10.1029/2011RG000376.

Serra, N., Ambar, I., and Boutov, D., 2010, Surface expression of Mediterranean water dipoles and their contribution to the shelf/slope–open ocean exchange: Ocean Science, v. 6, p. 191–209, doi:10.5194/os-6-191-2010.

Manuscript received 4 September 2013
Revised manuscript received 23 November 2013
Manuscript accepted 25 November 2013

Printed in USA

Appendix A. Supplementary Materials

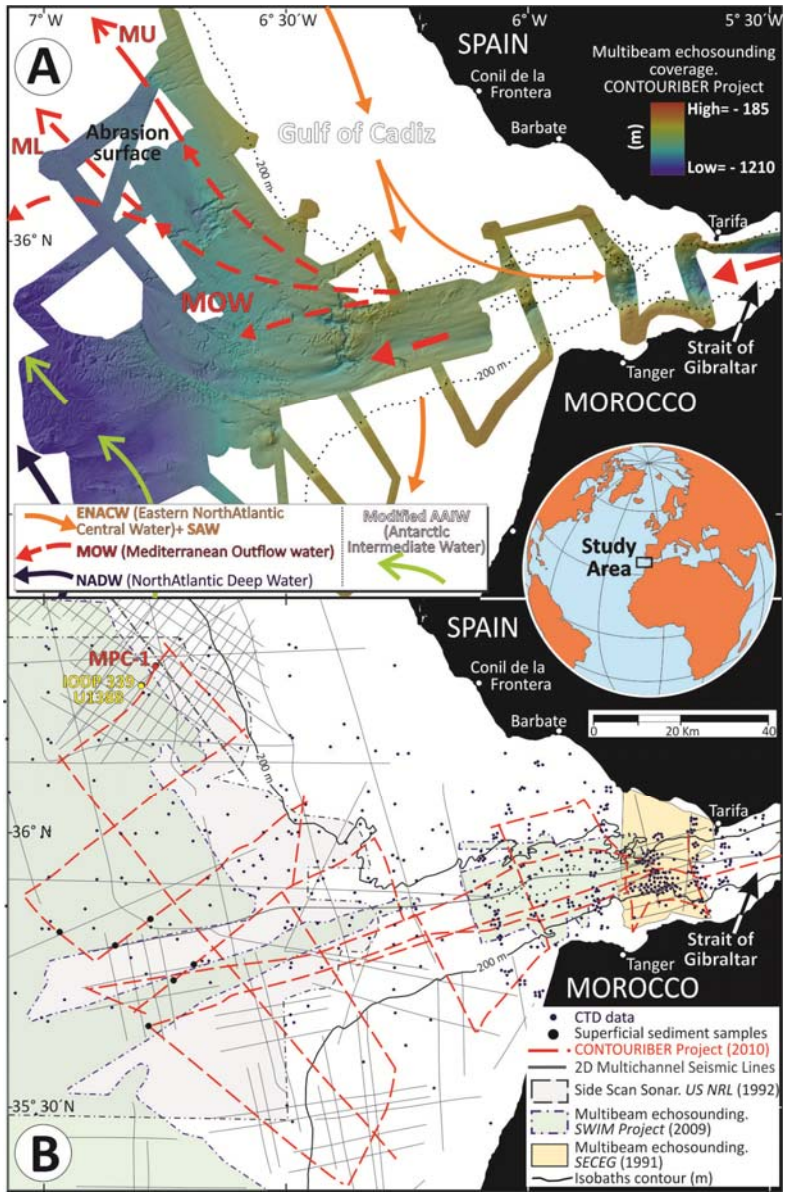

Figure DR1. Study area with the data sets (a and b) used in this work and the regional water-mass circulation sketched. The data that we used in this study were acquired mainly during the CONTOURIBER-1 Cruise (2010) onboard RV "Sarmiento de Gamboa" and include: I) swath bathymetry (showed in a); II) very high-resolution (Parasound) and mid-resolution (airgun) seismics; III) superficial sediment samples; and IV) Acoustic Doppler Current Profiler (ADCP) data. Published bathymetric data sets (showed in b) from the SWIM Project (Zitellini et al., 2009) were also utilized, including higher-resolution data from TV-GIB (Gutscher, 2005), the CADISAR-1 (Mulder et al., 2003) and Sonar-91 (IFREMER, 1991, SECEG/SNED) cruises, in addition to a regional geophysical compilation. Industry borehole MPC-1 (1982) provided details on margin evolution and age constraints. Finally, a very detailed hydrographic analysis was performed, based on: I) the ADCP data; II) an extensive Conductivity, Temperature and Depth (CTD) dataset collected by the Universities of Lisbon and Cádiz since 1970; III) an integrated acoustic analysis of the water column, conducted at the University of Bremen, for detection of water-mass interfaces, nepheloid layers and internal waves; and IV) numerical simulations of bottom temperature, salinity and currents, performed at the University of Hamburg.

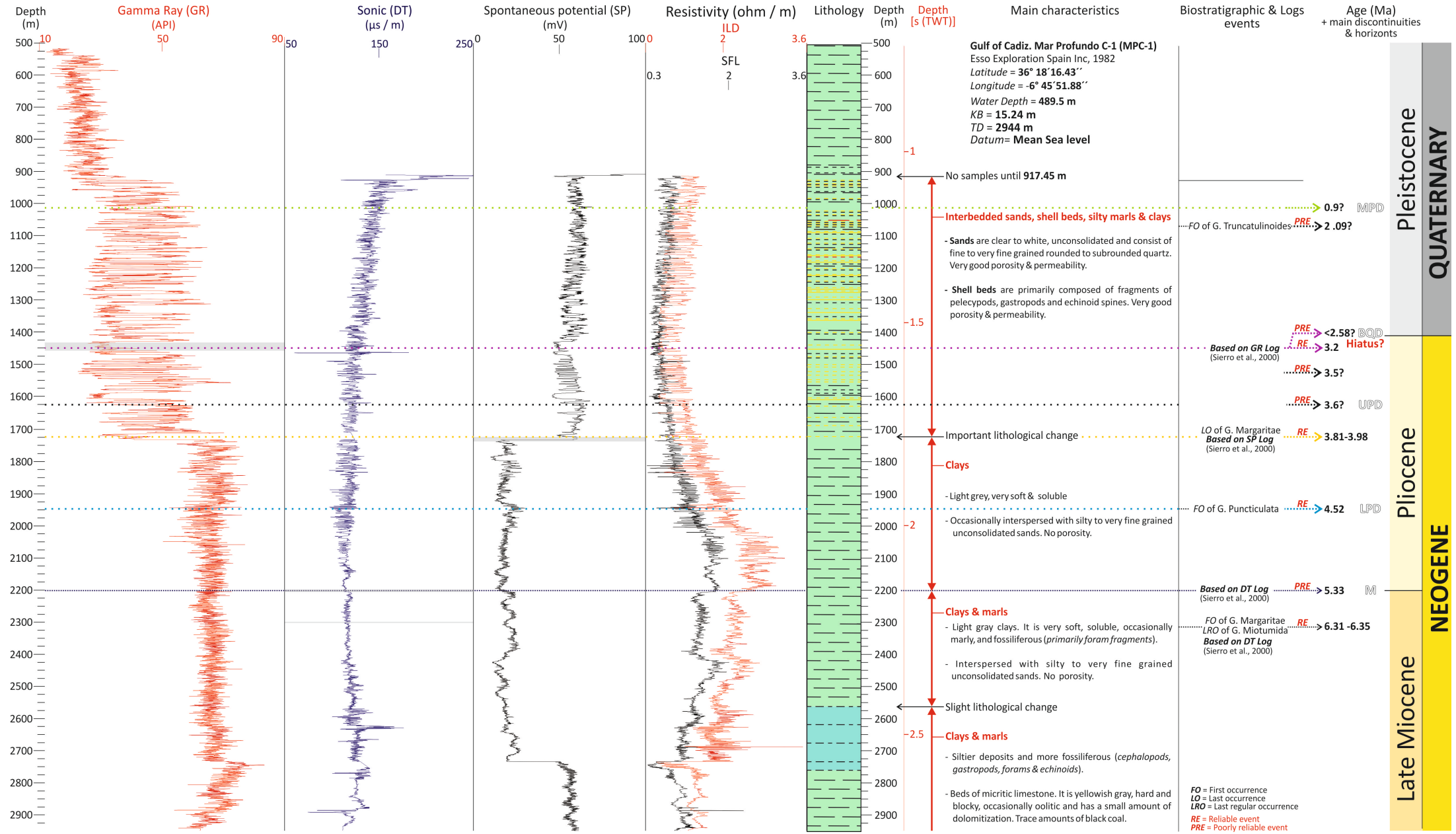

Figure DR2. Golfo de Cadiz, Mar Profundo C-1 (MPC-1, 1982) Borehole data showing the main lithologic and logging characteristics and the ages of the Miocene, Pliocene and Quaternary sedimentary records. The main discontinuities and stratigraphic horizons are included: Top of the Miocene (M); Lower Pliocene Reflection (LPR); Upper Pliocene Discontinuity (UPD); Base of the Quaternary (BQD); Mid Pleistocene Discontinuity (MPD). The chronology of the sediments was established based on the combination of planktonic foraminifera biostratigraphy performed in the sidewall samples taken along the borehole, and the cyclostratigraphic patterns defined in the well logs. The ages (in Ma) for the first occurrence (FO) and last occurrence (LO) of species are based on Lourens et al (2004). Additionally, patterns in the Gamma Ray (GR), Sonic (DT) and Spontaneous Potential (SP) were correlated with those previously defined by Sierro et al. (2000). A sandy/clayey interval is identified between 917 and 1722 m depth, with a porosity of 34 to 38% and the following main characteristics: sand-clay thickness of 815 m; net sand thickness of 600 m; net/total percentage of 74%; 80 reservoirs of sandy layers; average thickness of the frequent layer of 12 to 15 m; minimum layer thickness of 1.5 m; maximum layer thickness of 40 m; and net in layers of thickness higher than 10 m of 168 m (Buitrago et al., 2001).

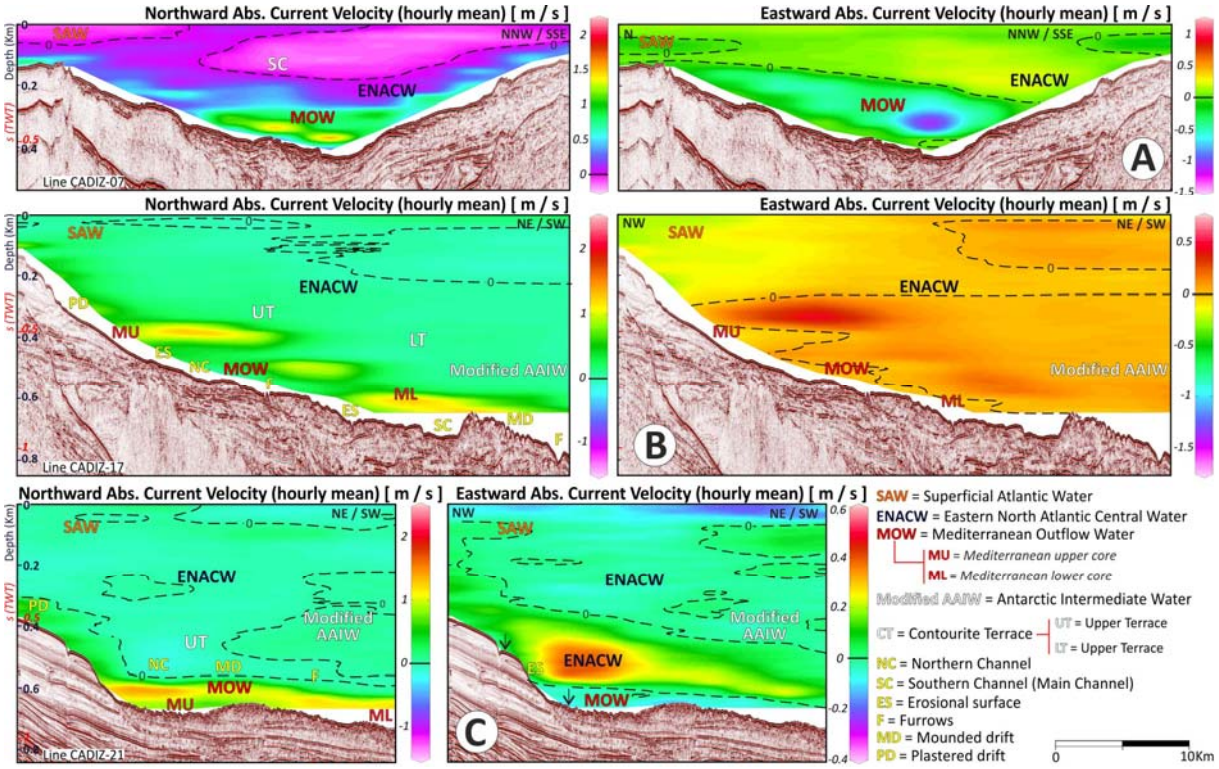

Figure DR3. Vertical sections of ocean velocity measured at the eastern area close to the exit of the Strait of Gibraltar (a) and further west (b and c). See Figure 1 for section locations. The water color code displays the Acoustic Doppler Current Profiler (ADCP) velocity components. Water-mass interpretations are shown on the left sections and major contourite features, on the right sections. The ocean velocities were measured by a 75 KHz hull-mounted ADCP. The panels on the left correspond to the velocity component in the east-west direction (positive values indicate currents towards the east), and the panels on the right correspond to the velocity component in the north-south direction (positive values indicate current towards the north). The dashed black lines indicate where the current velocity is zero.

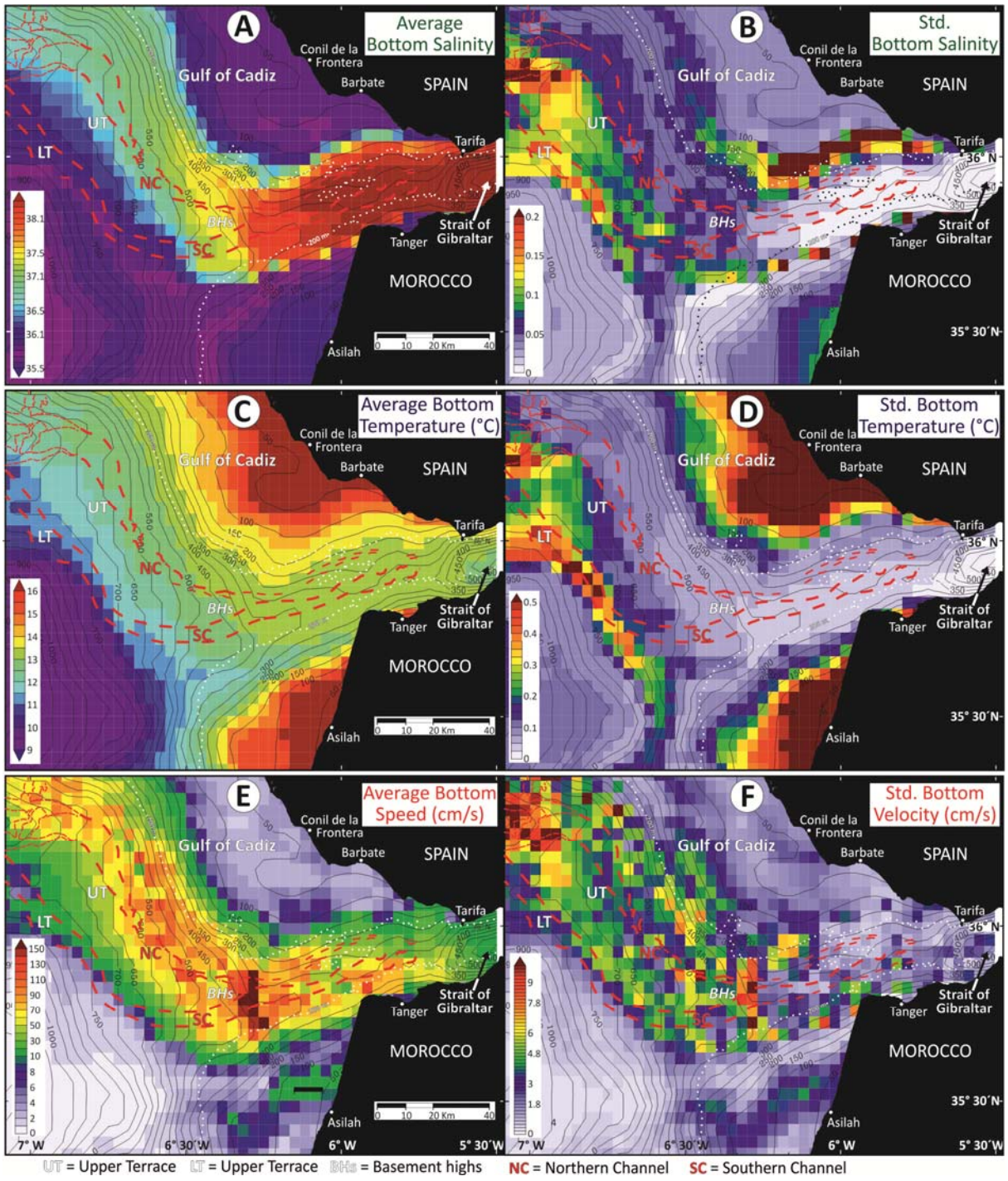

Figure DR4. Average (left) and standard deviation (right) of simulated bottom salinity (a,b), temperature (c,d) and speed (e,f) adjacent to the Strait of Gibraltar. Major erosional features (terraces and channels) are indicated. White dots represent the 200-m isobath. We used output of the MIT general circulation model (Marshall et al., 1997), configured to the Northeast Atlantic and Western Mediterranean regions from 9°E to 24°W and 30°N to 48°N with a horizontal resolution of about 2.8 km (Serra et al., 2010a). The vertical resolution varies from 5 m in the upper ocean to 100 m in the deep ocean (140 levels). The bottom topography was extracted from ETOPO2 and the initial temperature and salinity from the World Ocean Atlas 2005 (Boyer et al., 2005). The model was run for the period 1990 to 2009 forced at the surface by fluxes of momentum, heat and freshwater computed with bulk formulae and the NCEP reanalysis 6-hourly atmospheric state (Kalnay et al., 1996) and laterally by the output of a 16-km Atlantic solution of the MITgcm forced by the same NCEP dataset (Serra et al., 2010b). Vertical mixing uses the KPP formulation of Large et al. (1994) and Laplacian vertical diffusion and viscosity have coefficients of 1×10^{-4} m^2/s. A

quadratic bottom drag coefficient of 0.002 and biharmonic coefficients of horizontal diffusion and viscosity of 1×10^3 m^4/s and 5×10^8 m^4/s were employed. The simulation realism concerning the MOW circulation is discussed in Serra et al. (2010a). All analyses presented here were based on daily model output and corroborated our conclusion that, presently, the MOW flows mainly along the upper slope and the upper terrace (UT) in the middle slope, without any permanent circulation over the lower terrace (LT).

Table DR1. Regional characteristic values of potential temperature (θ), salinity (S), dissolved oxygen (O_2) and neutral density (γ^n) for the main water masses in the sector of the Gulf of Cadiz close to the Strait of Gibraltar.

Water Masses	**Temperature (T)** ° C	**Salinity (S)**	**Dissolved oxygen (O_2)** ml / l	**Neutral density (γ^n)** Kg / m^3
Surface Atlantic Water (SAW)	18-20	~36.4	4.6	1025.8-1026.3
East North Atlantic Central Water (ENACW)	10.6-16.5	35.6-36.3	5.06	1026.4-1027.6
Mediterranean Outflow Water (MOW)	13.1°	~38.5	4.15	1029.1
Modified Antarctic Intermediate Water (AAIW)	~10°	~35.62	~4.16	1027.5
(North) Atlantic Deep Water (NADW)	1.5-4°	34.8-35.2	5.52	1027.3-1027.9

REFERENCES

Boyer, T., Levitus, S., Garcia, H., Locarnini, R., Stephens, C., and Antonov, J., 2005, Objective analyses of annual, seasonal, and monthly temperature and salinity for the World Ocean on a 0.25° grid: International Journal of Climatology, 25(7), p. 931-945. doi:10.1002/joc.1173

Buitrago, J., García, C., Cajebread-Brow, J., Jiménez, A., and Martínez del Olmo, W., 2001, Contouritas: Un excelente almacén casi desconocido (Golfo de Cádiz, SO de España): 1er Congreso Técnico Exploración y Producción REPSOL-YPF, Madrid, p. 24-27.

Gutscher, M.A., 2005, Destruction of Atlantis by a great earthquake and tsunami?. A geological analysis of the Spartel Bank hypothesis: Geology, v. 33, p. 685-688, doi: 10.1130/G21597AR.1

Kalnay, E., Kanamitsu, M., Kistler, R., et al., 1996, The NCEP/NCAR 40-year reanalysis project: Bulletin of the American Meteorological Society, v. 77, p. 437-470, doi: 10.1175/1520-0477(1996)077<0437:TNYRP>2.0.CO;2

Large, W., McWilliams, J., and Doney, S., 1994, Ocean vertical mixing: A review and a model with a nonlocal boundary layer parameterization: Revews of Geophyisics, v. 32, p. 363-403, doi:10.1029/94RG01872

Lourens, L., Hilgen, F., Shackleton, N.J., Laskar, J., and Wilson, D., 2004, The Neogene period. *in* Gradstein, F.M., Ogg, J.G., and Smith, A., Eds., A Geologic Time Scale 2004: Cambridge (Cambridge Univ. Press), p. 409–440, http://dx.doi.org/10.1017/CBO9780511536045.022

Marshall, J., Adcroft, A., Hill, C., Perelman, L., and Heisey, C., 1997, A finite-volume, incompressible Navier Stokes model for studies of the ocean on parallel computers: Journal of Geophysical Research Oceans, v. 102, p. 5753-5766, doi:10.1029/96JC02775

Mulder, T., Voisset, M., Lecroart, P., Le Drezen, E., Gonthier, E., Hanquiez, V., Faugères, J.C., Habgood, E., Hernandez-Molina, F.J., Estrada, F., Llave, E., Poirier, D., Gorini, C., Fuchey, Y., Volker, A., Freitas, P., Lobo Sanchez, F., Fernandez, L.M., and Morel, J., 2003, The Gulf of Cadiz: an unstable giant contouritic levee: Geo-Marine Letters, v. 23, p. 7-18, doi: 10.1007/s00367-003-0119-0

Serra, N., Ambar, I., and Boutov, D., 2010a, Surface expression of Mediterranean Water dipoles and their contribution to the shelf/slope - open ocean exchange: Ocean Science, v. 6, p. 191-209, doi:10.5194/osd-6-2579-2009

Serra, N., Käse, R.H., Köhl, A., Stammer, D., and Quadfasel, D., 2010b, On the low-frequency phase relation between the Denmark Strait and the Faroe-Bank Channel overflows: Tellus, v. 62A, p. 530-550, doi:10.1111/j.1600-0870.2010.00445.x

Sierro, F.J., Ledesma, S., Flores, J.A., Torrescusa, S., and Martínez Del Olmo, W., 2000, Sonic and gamma-ray astrochronology: Cycle to cycle calibration of Atlantic climatic records to Mediterranean sapropels and astronomical oscillations: Geology, v. 28, p. 695-698, doi:10.1130/0091-7613(2000)28<695:SAGACT>2.0.CO;2

Zitellini, N., Gràcia, E., Matias, L., Terrinha, P., Abreu, M.A., DeAlteriis, G., Henriet, J.P., Dañobetia, J.J., Masson, D.G., Mulder, T., Ramella, R., Somoza, L., and Diez, S., 2009, The quest for the Africa-Eurasia plate boundary west of the Strait of Gibraltar: Earth and Planetary Science Letters, v. 280, p. 13–50, doi:10.1016/j.epsl.2008.12.005